

Effects of Gas Ion Density on Formation of Gas-Atom Encapsulated Silicon Fullerenes

Masahiro YABUNO, Toshiro KANEKO, and Rikizo HATAKEYAMA

Department of Electronic Engineering, Tohoku University, Aoba 6-6-05, Aoba-ku, Sendai 980-8579, Japan.

(Received: 19 September 2008 / Accepted: 5 January 2009)

Silicon (Si) cage clusters, i.e., Si fullerenes doped with argon (Ar) atom are formed using a Si plasma. The Si plasma is generated by irradiation of an electron beam to a Si lump in Ar gas atmosphere. When the Ar gas pressure is 0.08 Pa or more, the Ar plasma is also generated by the collision of the electron beam and superimposed upon the Si plasma. The ionized Si agglutinates in the diffusion process and agglutinated Si fullerenes are deposited on a substrate. The mass analysis of the Si fullerenes deposited on the substrate is performed using a laser-desorption time-of-flight mass spectrometer. As a result, the mass peaks of the Si fullerenes doped with the Ar atom, i.e., Ar encapsulated Si fullerenes are observed only under the condition that the Ar ions are generated in addition to the Si plasma. This result suggests that the Ar ions influence the formation of the Ar encapsulated Si fullerenes.

Keywords: silicon fullerene, silicon plasma, gas-atom encapsulation, electron beam

1. Introduction

Silicon (Si) cage clusters, i.e., Si fullerenes are expected as one of the electronic materials for future nano- and opto-electronics. *Ab initio* calculation works have theoretically indicated that the metal encapsulated Si fullerenes have high structural stability compared with the case of the pure Si fullerenes [1]. In addition, several experimental works about the formation of the metal encapsulated Si fullerenes have been reported [2 - 7]. Furthermore, it is calculated that Si fullerenes have advantageous characteristics, such as wide band gap and luminescence in an optical region [1]. Therefore, they can be applied to semiconductor and light emitting devices. However, the reports on the formation of the Si fullerenes are still few, and the encapsulated materials are limited to metal atoms [2 - 7]. In the case of carbon fullerenes such as C_{60} and C_{70} , on the other hand, not only the metal atoms but also noble gas atoms can be doped into carbon fullerenes [8 - 10], and the noble gas-atom encapsulated C_{60} has an improved property in the superconductivity compared with the case of pristine C_{60} [10]. On the basis of these results, in this study, we are trying to form gas-atom encapsulated Si fullerenes using a Si plasma. Since the gas atoms are easily ionized and a large amount of gas ions can affect the formation of the Si fullerenes, the high efficient formation of the atom encapsulated Si fullerenes is expected when suitable plasma technology is adopted for that purpose. Therefore, it is desired to develop a method for the formation of the Si fullerenes including the gas atoms in their cages.

In our experiment, the Si plasma is generated by irradiation of a high-energy electron beam to a Si lump in the solid phase [11]. To synthesize the Si fullerenes, an argon (Ar) plasma is also generated by the collision of the electron beam and superimposed upon the Si plasma. The ionized Si agglutinates and becomes cage-shaped clusters in the diffusion process. As a result, Ar atoms are encapsulated into the cage of Si fullerenes.

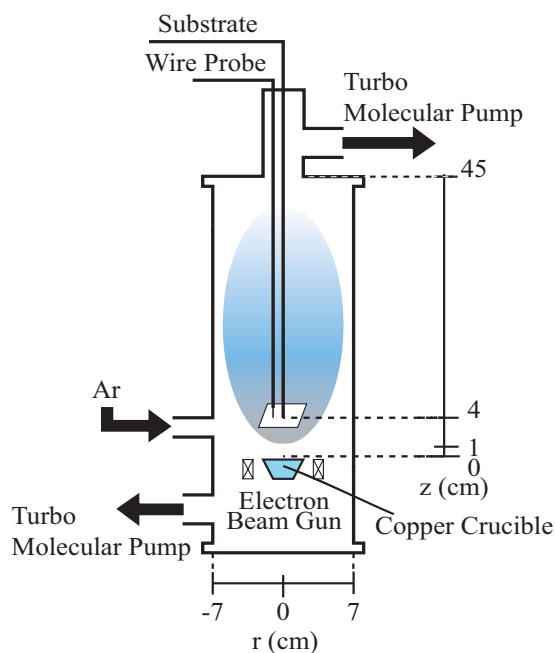


Fig.1 Schematic diagram of experimental setup.

author's e-mail: yabuno@plasma.ecei.tohoku.ac.jp

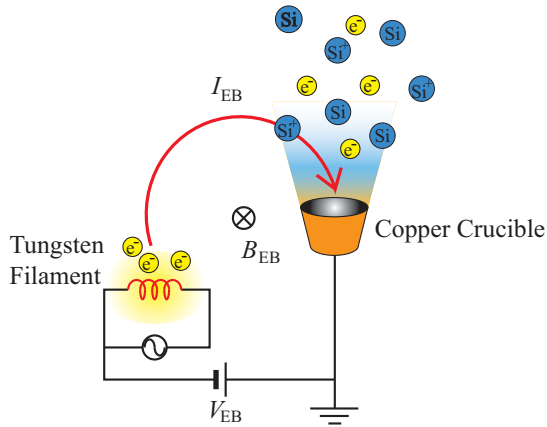


Fig.2 Principle of EB gun.

2. Experimental Apparatus

A schematic of experimental apparatus is shown in Fig. 1. The Si lump is set in a water-cooled copper crucible located at the axial position of $z = 0$ cm, and Si atoms from the lump are evaporated and ionized using an electron beam gun (EB gun; ANELVA, 980-7300). The EB gun can easily evaporate and ionize the Si which is a high boiling point material. Plasma parameters are measured by a Langmuir probe installed at $z = 1 - 4$ cm. A stainless substrate is set at $z = 4$ cm and electrically floated. The Si clusters that are formed during experiments are deposited on the substrate.

Figure 2 shows a principle of the EB gun. Thermionic electrons are emitted from a tungsten filament which is heated by applying an alternating-current power. The emitted thermionic electrons are accelerated by an electric field and deflected in a magnetic field by Lorentz force. The deflected electrons are irradiated toward the Si lump set in the copper crucible. Then, the Si is evaporated and ionized by the collision of the high-energy electron beam (4 - 5 keV).

The experimental conditions are as follows: background gas pressure $P \approx 10^{-4}$ Pa, Ar gas pressure $P_{\text{Ar}} = 0 - 0.5$ Pa, electron acceleration voltage of EB gun $V_{\text{EB}} = 4 - 5$ kV and electron emission current of the EB gun $I_{\text{EB}} = 25 - 150$ mA, which can determine the amount of Si evaporation.

The mass analysis of Si clusters deposited on the substrate is performed using a laser-desorption time-of-flight mass spectrometer (LD-TOF-MS; Shimadzu, AXIMA-CFR+). The Si clusters are detected as negative ions (negative ion mode) in LD-TOF-MS. Here, the deposited Si clusters are once taken out of the vacuum chamber, and are transferred to LD-TOF-MS.

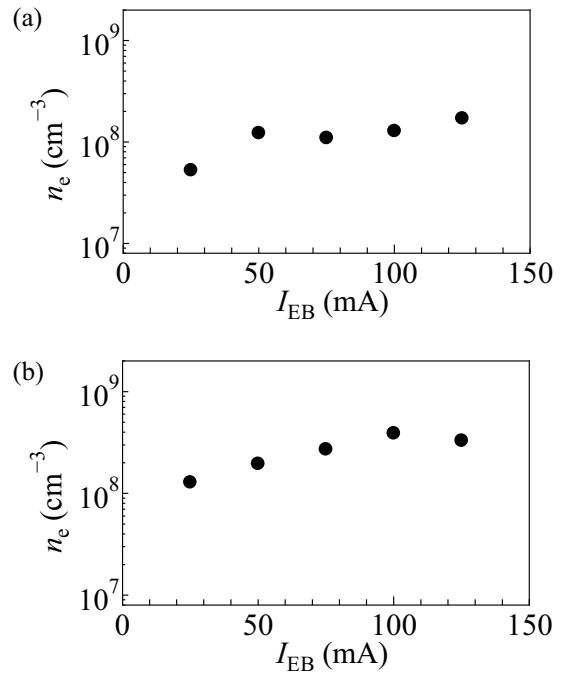


Fig.3 Electron density n_e as a function of electron beam current I_{EB} (a) for $P_{\text{Ar}} = 0$ Pa, and (b) for $P_{\text{Ar}} = 0.1$ Pa, where $z = 1$ cm and $V_{\text{EB}} = 4$ kV.

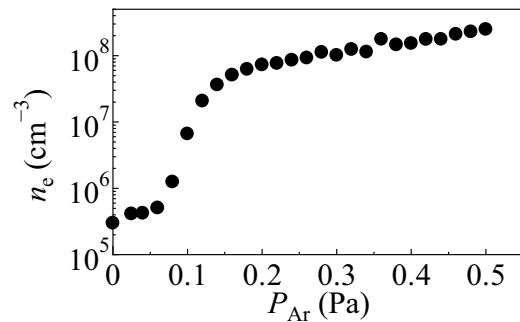


Fig.4 Electron density n_e as a function of Ar gas pressure P_{Ar} for $V_{\text{EB}} = 5$ kV, $I_{\text{EB}} = 50$ mA, and $z = 4$ cm.

3. Experimental Results

Figure 3 shows the electron density n_e as a function of electron beam current I_{EB} (a) for $P_{\text{Ar}} = 0$ Pa and (b) for $P_{\text{Ar}} = 0.1$ Pa, which is measured at $z = 1$ cm for $V_{\text{EB}} = 4$ kV. Since the Ar gas is absent under the condition in Fig. 3(a), the electron density denotes the Si ion density. The Si ion density gradually increases with an increase in I_{EB} , suggesting that the electron beam can evaporate and ionize Si, and the Si plasma is easily generated using the electron beam gun. In the case that the Ar gas is introduced, on the other hand, the electron density is larger than the case that Ar gas is absent, and increases with an increase in I_{EB} [Fig. 3(b)]. This is because the Ar plasma is generated by collisions of the electron beam with the Ar gas atoms.

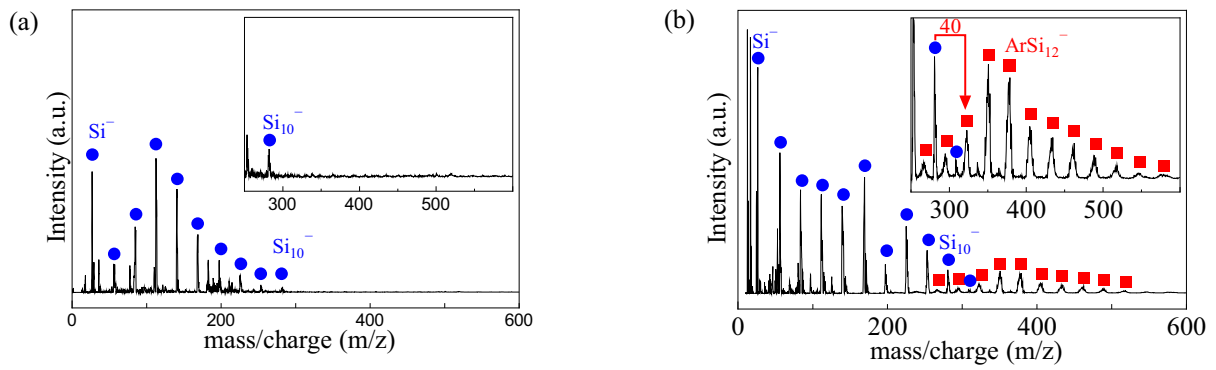


Fig.5 LD-TOF mass spectra of the Si clusters deposited on the substrate, which are produced by (a) the pure Si plasma for $V_{EB}=4$ kV, $I_{EB}=100$ mA, $P_{Ar}=0$ Pa, and deposition time $t=10$ min, and (b) the Si-Ar plasma for $V_{EB}=4$ kV, $I_{EB}=100$ mA, $P_{Ar}=0.3$ Pa, and $t=10$ min. The inset shows the magnification of the mass spectra in the range of 250-600 m/z .

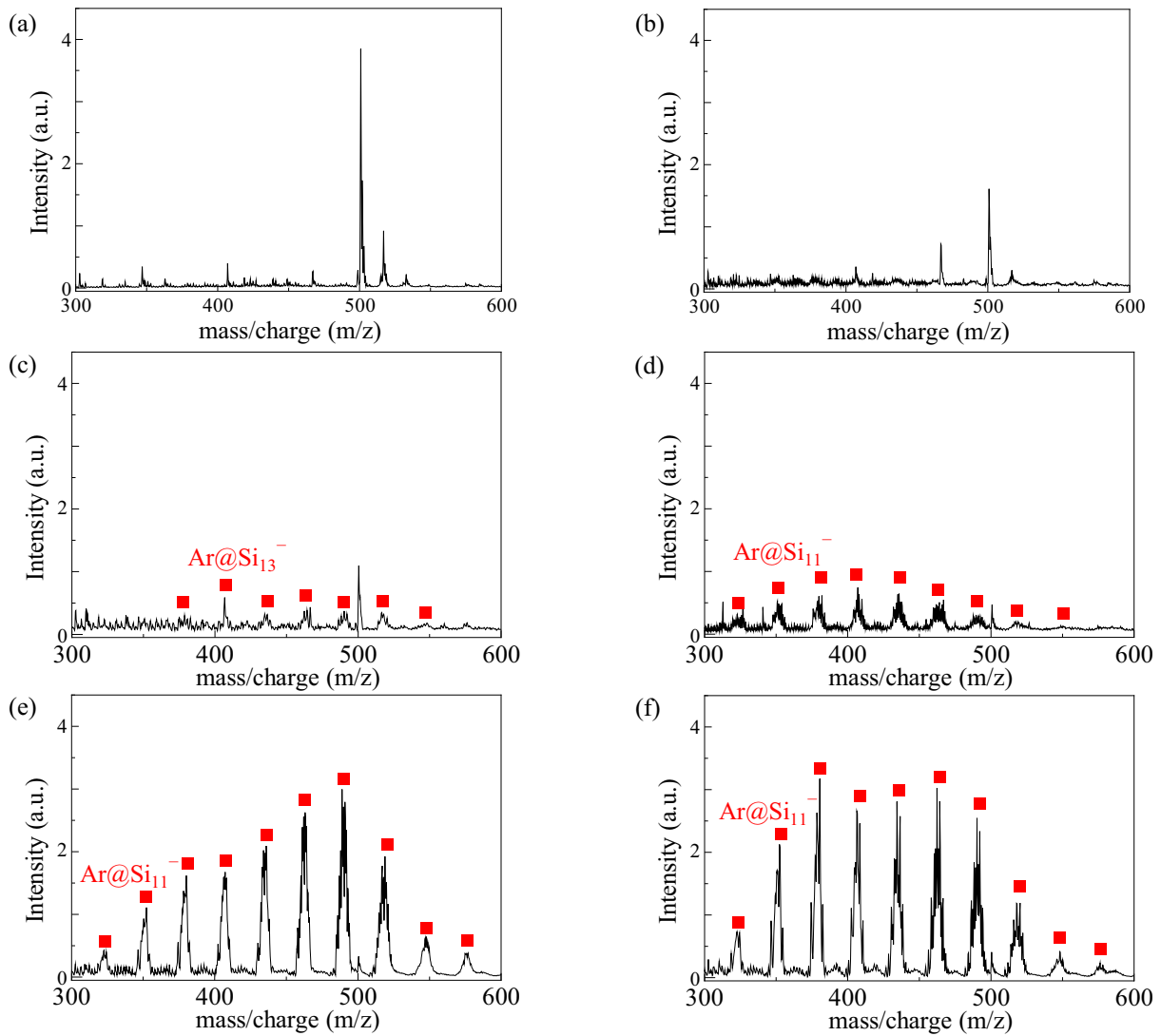


Fig.6 LD-TOF mass spectra of the Si fullerenes with Ar gas pressure P_{Ar} as a parameter for $V_{EB}=5$ kV, $I_{EB}=50$ mA, and $t=10$ min. (a) $P_{Ar}=0$ Pa, (b) $P_{Ar}=0.05$ Pa, (c) $P_{Ar}=0.08$ Pa, (d) $P_{Ar}=0.1$ Pa, (e) $P_{Ar}=0.3$ Pa, and (f) $P_{Ar}=0.5$ Pa.

Figure 4 displays the electron density n_e as a function of P_{Ar} for $V_{EB} = 5$ kV, $I_{EB} = 50$ mA, and $z = 4$ cm. It is found that n_e drastically increases when P_{Ar} exceeds about 0.06 Pa. This change of n_e represents the generation of the Si and Ar plasmas. For $P_{Ar} < 0.08$ Pa, only the Si plasma is generated. Under the condition $P_{Ar} \geq 0.08$ Pa, the Ar plasma starts to be generated. With increasing P_{Ar} , collisions of the electron beam with the Ar gas atoms increase, and the Ar ions are more generated.

Figure 5 gives typical LD-TOF mass spectra of the Si clusters deposited on the substrate, which are formed by (a) the pure Si plasma for $V_{EB} = 4$ kV, $I_{EB} = 100$ mA, $P_{Ar} = 0$ Pa, and deposition time $t = 10$ min, and (b) the Si–Ar plasma for $V_{EB} = 4$ kV, $I_{EB} = 100$ mA, $P_{Ar} = 0.3$ Pa, and $t = 10$ min. In the case of using the pure Si plasma [Fig. 5(a)], the mass peaks of the Si nano-clusters Si_n with $n = 1 - 10$ are clearly observed every 28 m/z, which are labeled by closed circles. In the case of using the Si–Ar plasma [Fig. 5(b)], on the other hand, the Si clusters having mass numbers larger than the pure Si nano-clusters by 40 m/z are observed in the high mass number region in addition to the pure Si nano-clusters Si_n ($n = 1 - 13$). This mass number shift is considered to be attributed to the addition of Ar to the Si clusters [11]. The mass peaks of the Si clusters doped with Ar atom ($ArSi_n$; $n = 8 - 20$) are labeled by the closed squares. The Si clusters doped with Ar atom formed in this experiment consist of Si atoms more than eight. And, it is predicted that the Si cluster composed of eight atoms or more has the cage structure. Based on these results, it is thought that $ArSi_n$ ($n \geq 8$) has the cage structure, in other words, $ArSi_n$ may be Ar encapsulated Si fullerenes ($Ar@Si_n$).

Figure 6 shows LD-TOF mass spectra of the Si fullerenes doped with Ar atom with P_{Ar} as a parameter for $V_{EB} = 5$ kV, $I_{EB} = 50$ mA, and $t = 10$ min. In all the cases, the pure Si nano-clusters are formed in the same manner as the case of $P_{Ar} = 0$ Pa as shown in Fig. 5(a). When we focus on the $Ar@Si_n$, the mass peaks of $Ar@Si_n$ are observed in the case of $P_{Ar} \geq 0.08$ Pa, where the Si–Ar plasma is generated as shown in Fig. 4. However, in the case of $P_{Ar} < 0.08$ Pa where the Ar plasma is not generated, the mass peaks of $Ar@Si_n$ are not observed.

Figure 7 shows the mass peak intensity ratio of $Ar@Si_n$ to Si_n as a function of P_{Ar} . The mass peak intensity ratio $Ar@Si_n/Si_n$ is calculated in the following formula:

$$\frac{Ar@Si_n}{Si_n} = \frac{Ar@Si_8 + Ar@Si_9 + \dots + Ar@Si_{20}}{Si_1 + Si_2 + \dots + Si_{10}} \times 100.$$

The mass peak intensity ratio $Ar@Si_n/Si_n$ increases with an increase in P_{Ar} . As shown in Fig. 4, there exists the threshold that the Ar plasma begins to be generated between $P_{Ar} = 0.06$ Pa and 0.08 Pa, and additionally, the Ar ion density gradually increases with an increase in P_{Ar} . This situation accords with Figs. 6 and 7. These results suggest the possibility that existence of the Ar ions near the

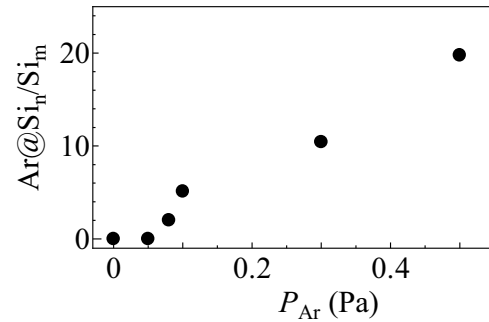


Fig.7 Mass peak intensity ratio of $Ar@Si_n$ for Si_n as a function of P_{Ar} .

Si plasma source enhances the formation of the Si cage clusters doped with Ar atom, namely, Ar encapsulated Si fullerenes.

4. Conclusions

When a Si plasma is generated by a high-energy electron beam, the silicon nano-clusters (Si_n ; $n = 1 - 13$) are found to be formed from a solid Si source. Furthermore, when Ar ions are generated in addition to the Si plasma, the Si cage clusters doped with Ar atom, i.e., Ar encapsulated Si fullerenes ($Ar@Si_n$; $n = 8 - 20$) are demonstrated to be formed. $Ar@Si_n$ begins to be formed when the Ar gas pressure exceeds 0.06 Pa, which corresponds to the threshold that the Ar plasma starts to be generated. In addition, the intensity of the mass peaks of $Ar@Si_n$ increases with an increase in P_{Ar} .

Acknowledgements

The authors are indebted to H. Ishida for his technical assistance. They thank the members of Technical Division, School of Engineering, Tohoku University for their technical support in laser-desorption time-of-flight mass spectrometry. This work was supported by a Grant-in-Aid for Scientific Research from the Ministry of Education, Culture, Sports, Science and Technology, Japan.

- [1] V. Kumar and Y. Kawazoe: Phys. Rev. Lett. **87**, 045503 (2001).
- [2] S. M. Beck: J. Chem. Phys. **90**, 6306 (1989).
- [3] H. Hiura, T. Miyazaki, and T. Kanayama: Phys. Rev. Lett. **86**, 1733 (2001).
- [4] A. Negishi, N. Kariya, K. Sugawara, I. Arai, H. Hiura and T. Kanayama: Chem. Phys. Lett. **388**, 463 (2004).
- [5] M. Ohara, K. Koyasu, A. Nakajima, and K. Kaya: Chem. Phys. Lett. **371**, 490 (2003).
- [6] A. Pramann, K. Koyasu, A. Nakajima, and K. Kaya: International of mass spectrometry. **229**, 77 (2003).
- [7] S. H. Huh, A. Nakajima, and K. Kaya: J. Appl. Phys. **95**, 2734 (2004).

- [8] M. Saunders, H. A. Jimenez-Vazquez, R. J. Cross, S. Mroczkowski, D. I. Freedberg, and F. A. L. Anet: *Nature (London)* **367**, 256 (1994).
- [9] M. S. Syamala, R. J. Cross, and M. Saunders: *J. Am. Chem. Soc.* **124**, 6216 (2002).
- [10] A. Takeda, Y. Yokoyama, S. Ito, T. Miyazaki, H. Shimotani, K. Yakigaya, T. Kakiuchi, H. Sawa, H. Takagi, K. Kitazawa, and N. Drago: *Chem. Commun.* **912**, (2006).
- [11] T. Kaneko, H. Takaya, and R. Hatakeyama: *Appl. Phys. Lett.* **89**, 241501 (2006).